

Progressive Text-to-Image Generation

Zhengcong Fei, Mingyuan Fan, Li Zhu, Junshi Huang*
Meituan
Beijing, China
{name}@meituan.com

arXiv:2210.02291v5 [cs.CV] 20 Sep 2023

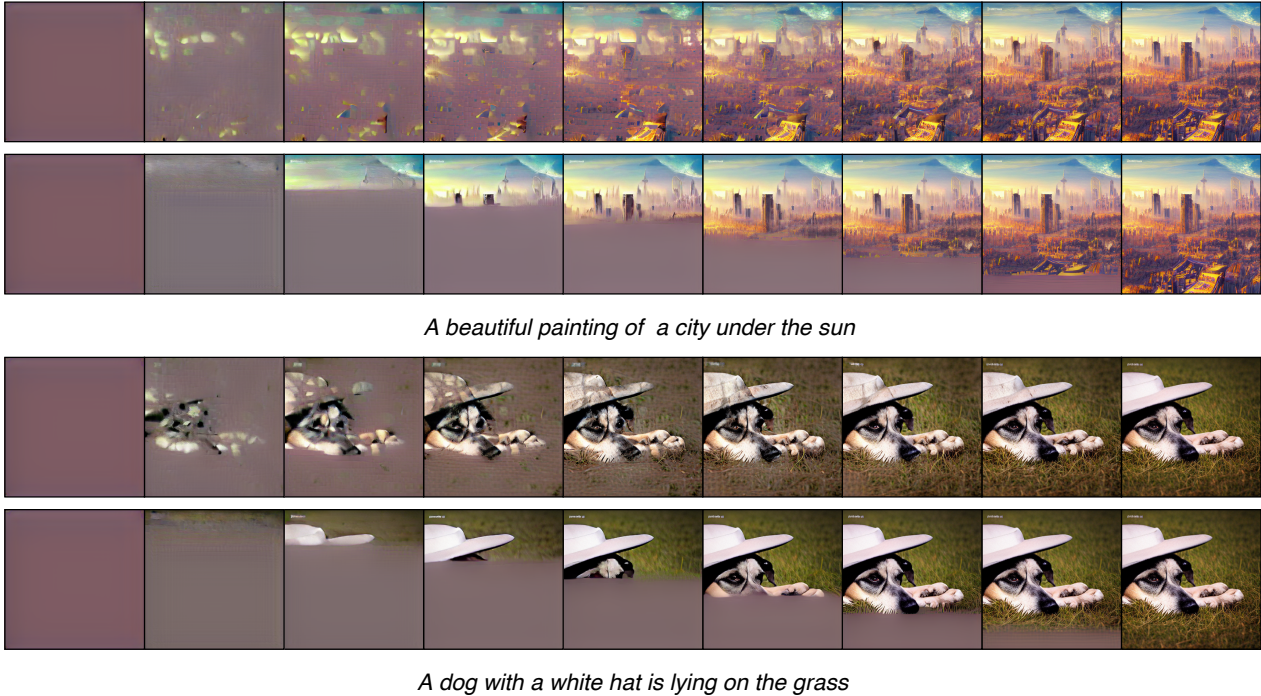


Figure 1. Illustration of different generation orders for text-to-image synthesis. Conventional model generates vector quantized image sequence *from left to right* as top, while our progressive model creates image patches *from coarse to fine* as bottom.

Abstract

Recently, *Vector Quantized AutoRegressive (VQ-AR)* models have shown remarkable results in *text-to-image synthesis* by equally predicting discrete image tokens from the top left to bottom right in the latent space. Although the simple generative process surprisingly works well, is this the best way to generate the image? For instance, human creation is more inclined to the *outline-to-fine* of an image, while VQ-AR models themselves do not consider any relative importance of image patches. In this paper, we present a progressive model for high-fidelity text-to-image generation. The proposed method takes effect by creating new image tokens from coarse to fine based on the existing context

in a parallel manner, and this procedure is recursively applied with the proposed error revision mechanism until an image sequence is completed. The resulting coarse-to-fine hierarchy makes the image generation process intuitive and interpretable. Extensive experiments in MS COCO benchmark demonstrate that the progressive model produces significantly better results compared with the previous VQ-AR method in FID score across a wide variety of categories and aspects. Moreover, the design of parallel generation in each step allows more than $\times 13$ inference acceleration with slight performance loss.

1. Introduction

The task of text-to-image generation aims to create natural and consistent images from the input text and has received extensive research interest. Recently, latent autoregressive (AR) generation frameworks have achieved great success in advancing the start-of-the-arts, by learning knowledge and patterns from a large-scale multimodal corpus [35, 42, 64]. Generally, they treat the task as a form of language modeling and use Transformer-like [59] architectures to learn the relationship between language inputs and visual outputs. A key component of these approaches is the conversion of each image into a sequence of discrete units through the use of a VQ-VAE [57] based image tokenizer, *e.g.*, VQ-GAN [16, 63], RQ-VAE [32] and ViT VQ-GAN [63]. Visual tokenization essentially unifies the view of text and images so that both can be treated simply as sequences of discrete tokens and is adaptable to sequence-to-sequence models. To that end, DALL-E [47], CogView [12], RQ-Transformer [32], and Parti [65] employ autoregressive models to learn text-to-image task from a large collection of potentially noisy text-image pairs [5, 17, 27]. In particular, [62] further expand on this AR over AR modeling approach to support arbitrarily-sized image generation.

Another research line for text-to-image generation involves diffusion-based methods, such as GLIDE [38], DALL-E 2 [46], stable diffusion [49], RQ-Transformer [32], and Imagen [51]. These models pursue to directly generate images or latent image features with diffusion process [11, 22] and produce high-quality images with great aesthetic appeal. Even so, discrete sequence modeling for text-to-image generation remains appealing given extensive prior work on large language models [4] and advances in discretizing other modalities, such as video and audio, as cross-language tokens [3]. However, the current constructed plain and equal paradigm, without enough global information [56], may not reflect the progressive hierarchy/granularity from high-level concepts to low-level visual details and is not in line with the actual human image creation. Also, the time complexity of standard auto-regressive image sequence generation is $\mathcal{O}(n)$, which meets a critical limitations for high resolution image generation.

Motivated by the above factors, we present the *progressive model* for text-to-image generation from coarse to fine. Specifically, it takes text tokens as inputs to an encoder and progressively predicts discrete image tokens with a decoder in the latent space. The image tokens are then transformed by the VQ-GAN decoder, which can produce high-quality reconstructed outputs. As illustrated in Figure 1, given text prompts, our model first generates high-level content skeleton, then these information are used as pivoting points according to which to create the details of finer granularity. This process iterates until an image is finally completed by adding the fine-grained tokens. Meanwhile, the error tokens

generated in previous steps can be *dynamically* revised as more details are filled. We show that such progressive generation in a latent space is an effective and efficient way to improve text-to-image performance, enabling to accurately integrate and visually convey world knowledge.

To evaluate the framework, we conduct text-to-image generation experiments on the popular MS COCO [37] benchmark. Compared with the convention AR model with similar model parameters, our method achieves significantly better image generation performance, as measured by image quality and image-text alignment in both automatic metrics and human evaluations. The progressive model also provides important benefits for the inference speed. As the inference time of AR methods increases linearly with the output image resolution, the progressive model provides the global context for image token prediction and employs the importance score for parallel set selection. This allows us to provide an effective way to achieve a better trade-off between the inference speed and the image quality. We hope this technique can help visual content creators to save time, cut costs and improve their productivity and creativity.

Finally, we summarize the contributions of this paper as follows: **(i) Order matters.** We argue that the importance of image tokens is not equal and present a novel progressive model in the VQ-based latent space for text-to-image generation. Compared with previous work, our method allows long-term control over a generation due to the top-down progressive structure and enjoys a significant reduction over empirical time complexity. **(ii)** We use large-scale pre-training and *dynamic error revision* mechanism customized to our approach, to further boost image generation performance. **(iii)** Experiments on the dataset across different aspects demonstrate the superiority of progressive model over strong baselines. In particular, our approach is simple to understand and implement, yet powerful, and can be leveraged as a building block for future text-to-image synthesis research.

2. Background

We first briefly introduce the conventional vector quantized autoregressive model for text-to-image generation. Specifically, the two-stage process includes: **(i)** training an image tokenizer that turns an image into a sequence of discrete visual tokens for training and reconstructs the image at inference time and **(ii)** optimizing a sequence-to-sequence Transformer model that produces image tokens from text tokens in the latent space.

Image Tokenizer. Since the computation cost is quadratic to the sequence length, it is limited to directly modeling raw pixels using transformers [6]. Previous works [57, 63] addressed this by using a discrete variational auto-encoder (VAE), where a visual codebook is learned to map a patch



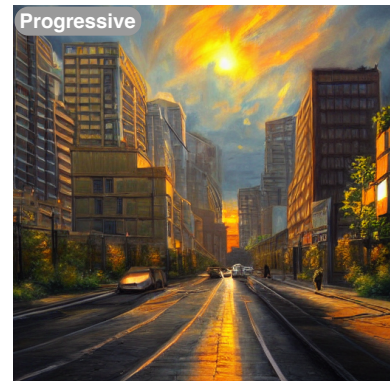
the end of the world



a teddy bear on a skateboard in times square



a dolphin travel on the saturn



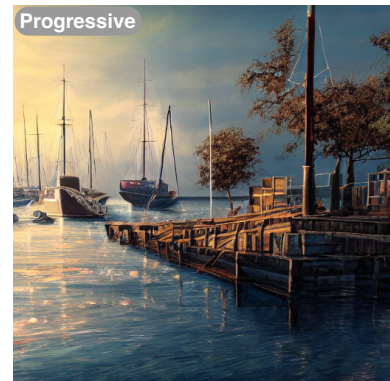
urban agglomerations in the setting sun



a white cute dog wearing a black hat



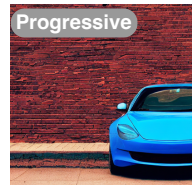
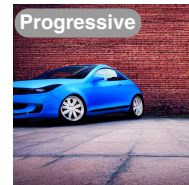
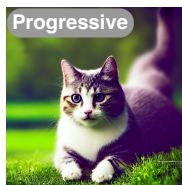
a couple of glasses are sitting on a table



painting of boats docked in a harbor



a cat playing in a green field next to a lake



a blue car parked in front of a yellow brick wall

Figure 2. Selected image samples generated from the progressive model and corresponding text prompts. Refer to Sec 4.3 for a more detailed discussion.

embedding to its nearest codebook entry in the latent space. These entries can be considered as visual words, and the appearance of these words of a given image are thus contained image tokens like words in a sentence. A VQ-VAE image tokenizer usually follows an encoder-decoder paradigm and is trained with the losses as [16] on the unlabeled images of training data. Specifically, the encoder E , the decoder D and the codebook $Z \in \{z_k\}_{k=1}^K$, where K is the code size, can be trained end-to-end via the following loss with training image I :

$$L_{vae} = \|I - \tilde{I}\|_1 + \|\text{sg}[E(I) - z_q]\|_2^2 + \beta \|\text{sg}[z_q] - E(I)\|_2^2, \quad (1)$$

where \tilde{I} is reconstructed image from $D(z_q)$ and z_q is the indexed embedding from codebook Z , that is,

$$z_q = Q(z) = \underset{z_k \in Z}{\text{argmin}} \|z - z_k\|_2^2, \quad (2)$$

$z = E(I)$ and $Q(\cdot)$ is mapping function from spatial feature z to z_q . $\text{sg}[\cdot]$ stands for the stop-gradient operation. In practice, we use VQ-GAN [16] with techniques including factorized codes and real-false discriminator for perception loss and exponential moving averages to update the codebook entries which contribute to training stability and reconstruction quality.

Text-to-Image Transformer. After unified image and text modalities with discrete tokens, a standard encoder-decoder Transformer model is then trained by treating text-to-image generation as a sequence-to-sequence modeling problem. The Transformer model takes text prompt as input and is trained using next-token prediction of image latent codes supervised from the image tokenizer. Formally, provided with text prompt X , the optimization objective for modeling of image token sequence $Y = \{y_1, \dots, y_L\}$ in training dataset \mathcal{D} can be factorized as:

$$L_{ar} = -\log p(Y|X) = -\log \prod_{i=1}^L p(y_i | y_{<i}, X). \quad (3)$$

During inference, the model samples image tokens autoregressively conditioned on the history context, which are later decoded into pixels using the VQ-GAN decoder to create the output image. For the text encoder, we load a pre-trained BERT-like model [29, 45] for training acceleration, and the decoding part of image tokens is trained from random initialization. Most of the existing latent-based text-to-image generation models can be split as decoder-only [12, 47], encoder-decoder [65] and diffusion models [20, 34, 49, 61] in the VQ-VAE based latent space. In this paper, we choose to focus on the encoder-decoder pattern with pre-trained text encoding.

3. Methodology

3.1. Overview

Provided with a text prompt X , we aim to generate a complete image token sequence \tilde{Y} , based on which the reconstructed image from VQ-GAN is accordingly high fidelity and semantically correlative to X . The generation procedure of our method can be formulated as a progressive sequence generation of T stages: $\tilde{Y} = \{\tilde{Y}^1, \dots, \tilde{Y}^T\}$, such that the predicted \tilde{Y}^{t+1} at $t+1$ -th stage preserves a finer-resolution image sequence compared to the sequence $\tilde{Y}^{\leq t}$ at preceding stages. In between, the intermediate state is formed as $\tilde{Y}^t = \{\tilde{y}_1^t, \dots, \tilde{y}_L^t | \tilde{y}_i^t \in \mathcal{V}\}$ and the corresponding token state sequence $\tilde{Z}^t = \{\tilde{z}_1^t, \dots, \tilde{z}_L^t | \tilde{z}_i^t \in \{0, 1, -1\}\}$, where \mathcal{V} is a VQ code vocabulary, and L is the image sequence length. The state sequence $\{0, 1, -1\}$ indicate that the token at each position of the intermediate sequence is unchanged, to be generated, or to be replaced, respectively. Formally, the i -th image token in the intermediate sequence of $(t+1)$ -th stage can be further formulated as $(1 - |\tilde{z}_i^{t+1}|)\tilde{y}_i^t + |\tilde{z}_i^{t+1}|\tilde{y}_i^{t+1}$.

Image Sequence Prediction. To generate the full sequence of image tokens within T stages, we constraint that $\forall t, \sum_{i=1}^L \mathbb{I}[\tilde{z}_i^t = 1] = \frac{L}{T}$. Therefore, the generation procedure with T stages can be modeled with factorized conditional probability as:

$$p(\tilde{Y}|X) = \prod_{t=1}^T \prod_{i=1}^L p(\tilde{y}_i^{t+1} | \tilde{Y}^t, X, \tilde{z}_i^{t+1}) p(\tilde{z}_i^{t+1} | \tilde{Y}^t, X, \tilde{Z}^t). \quad (4)$$

At each generation step t , model first produces the state sequence \tilde{Z}^{t+1} for the selection of to-be-updated token positions by $p(\tilde{z}_i^{t+1} | \tilde{Y}^t, X, \tilde{Z}^t)$. Once the changeable image token positions are determined, the corresponding tokens are generated or replaced according to distribution $p(\tilde{y}_i^{t+1} | \tilde{Y}^t, X, \tilde{Z}^{t+1})$, leading to a new image token sequence \tilde{Y}^{t+1} . Thus, we can recover the final image token sequence $P(\tilde{Y}|X)$ by marginalizing all the intermediate sequences. Note that such generation procedure starts from a fully masked image sequence $\{[mask], \dots, [mask]\}$ of length L , and then iteratively generate or revise the image tokens according to the predicted state sequence. Finally, this procedure terminates and outputs final image token sequence \tilde{Y}^T after T steps.

3.2. Progressive Image Generation

Two properties are desired for a progressive generation: *i*) important and outline tokens should appear in an earlier stage, so that the generation follows a coarse-to-fine manner; *ii*) the number of stages T should be small enough, thus the generation maintains fast at inference procedure. To this end, the key points of the progressive model lie in

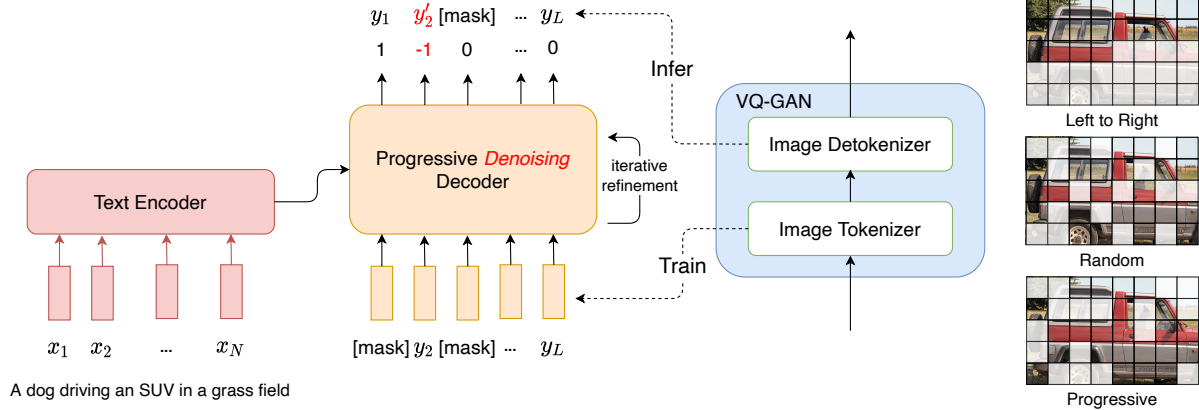


Figure 3. Overview of the proposed progressive text-to-image model, with left-to-right, random, and coarse-to-fine generation orders in the VQ-GAN latent space. Red symbols denote the error revision process.

the importance scores of image tokens for the determination of token generation order at each stage, as shown in Figure 3. In the following paragraphs, we introduce two variants for image token scoring, instead of random selection.

Quantization Error based Scoring. As the quantization error of VQ-GAN reflects the difficulty of image patch discretization, we can decide the generation order of tokens according to the quantization error of image tokens via VQ-GAN. Intuitively, the smaller the quantization error, the higher the quality and confidence of image to be reconstructed, and thus it is better to be generated at earlier stage. To this end, we obtain the quantization error sequence $E = \{e_1, \dots, e_L\}$ for image sequence $Y = \{y_1, \dots, y_L\}$ with the encoder of VQ-GAN. At t -th step, we collect the index set of top- $\frac{t}{T}L$ smallest values in error sequence E , according to which the value of z_i^t in state sequence Z^t is set as 1 if the i -th position belongs to the collected index set. Note that the values of Z^t are initialized as 0. Accordingly, the image token sequences $Y = \{Y_1, \dots, Y_T\}$ can be constructed like the state sequences $Z = \{Z^1, \dots, Z^T\}$, and we set $Y^0 = \{[mask], \dots, [mask]\}$ of length L .

Thereafter, the training instance (X, Y) can be broken into the consecutive series of training tuples $((X, Y^{t-1}), (Z^t, Y^t))$ for $t \in [1, T]$, where (X, Y^{t-1}) and (Z^t, Y^t) are the model input and ground-truth label at t -th stage, respectively. Then, we can train the confidence-aware generation model based on T series of training tuples by maximizing $\prod_{i=1}^L p(\tilde{y}_i^{t+1}|Y^t, X, z_i^{t+1})p(\tilde{z}_i^{t+1}|Y^t, X, Z^t)$ at each stage. In this way, the image tokens with high-confidence are generated at earlier stages, which may serve as the outline of image. After that, the model can leverage more context information for the generation of uncertain image tokens at following stages. As shown in Sec. 4.2, this simple yet powerful scoring strategy learned from pre-

defined confidence information presents promising result.

Dynamic Importance Scoring. We further propose to learn a dynamic scoring function for individual image token. In general, the model determines the image token generation order by sampling $\frac{t}{T}$ available positions at each stage, and maximizes a global reward function at final. In this case, we refer to the position selection as a policy $\pi_\theta(a_t|s_t)$, where an agent state s_t is $(\tilde{Y}^{\leq t}, X, \tilde{Z}^{\leq t})$. Note that we consider the entire trajectories of intermediate image sequences and state sequences, *i.e.*, $\tilde{Y}^{\leq t}$ and $\tilde{Z}^{\leq t}$, before and at current t -th stage in agent state. The action $a_t \in \{1, \dots, L\}^{\frac{t}{T}}$ is an intermediate set, so that the value of \tilde{Z}_i^{t+1} is 1 if $i \in a_t$, otherwise 0. Please note that a_t is sampled without replacement, and π_θ is simply a neural network. At the beginning, the agent state $s_1 = (\tilde{Y}^0, X, \tilde{Z}^0)$, where \tilde{Y}^0 and \tilde{Z}^0 are initialized as aforementioned. Then, we implement the generation process by repeatedly sampling the action $a_t \sim \pi_\theta(s_t)$ and transiting to a new agent state s_{t+1} for T steps. Meanwhile, we update the predicted image token sequence \tilde{Y}^{t+1} according to the updated state sequence \tilde{Z}^{t+1} at each $t+1$ stage. At the final stage, a scalar reward function r , *e.g.*, L2 loss for image reconstruction [14] or CLIP-based similarity [42], is used to find an optimal policy that maximizes the expected global reward. This procedure is equivalent to minimize the loss function:

$$L_{dis} = -E_{\tau \sim \pi_\theta(\tau)}[r(s_T)], \quad (5)$$

$$\pi_\theta(\tau) = p(s_1) \prod_{t=1}^T p(s_{t+1}|a_t, s_t) \pi_\theta(a_t|s_t), \quad (6)$$

where τ is the trajectory $(s_t, a_t, \dots, s_T, a_T)$, $p(s_1)$ is a deterministic value, and $p(s_{t+1}|a_t, s_t)$ is the generation model to update the image token sequence \tilde{Y}^{t+1} according to the state sequence \tilde{Z}^{t+1} decided by action a_t . In practice, we

maximize the reward function by estimating its gradient using the policy gradient [54] strategy.

3.3. Image Token Revision

Although the preceding progressive training makes the model capable of generating image sequences from coarse to fine, the model cannot alleviate the adverse impact of error tokens from earlier stages. Particularly, the new image tokens at each stage are simultaneously generated based on the prior context in our paradigm, without considering the information of each other. Such approach suffers from a conditional independence problem like non-autoregressive generation [18, 19]. Therefore, it is prone to generate repeated or inconsistent tokens at each generation stage.

To alleviate this problem, we propose an error revision strategy by *injecting pseudo error tokens* into the training data, and helps the model to recover from error tokens generated in previous stages. Formally, given the training tuple $((X, Y^{t-1}), (Y^t, Z^t))$, we randomly replace part of image tokens in Y^{t-1} with the tokens from other images, except for *[mask]* token. Meanwhile, the values at corresponding positions of state sequence Z^t are set as -1, which means to-be-updated. To avoid the misleading caused by too many pseudo error tokens, we randomly select some training tuples of each instance by Bernoulli(p_{error}) for pseudo data generation. In this way, we construct a new training data \mathcal{D} with those re-built pseudo tuples.

4. Experiments

In this section, we conduct the experiments to validate the effectiveness of our progressive model. Specifically, we compare with some state-of-the-art approaches in Sec 4.1, and conduct some ablation studies in Sec 4.2. Finally, we present some text-to-image cases in Sec 4.3, and human evaluation in Sec 4.4.

The architecture of progressive model almost follows VQ-GAN [16] and standard encoder-decoder Transformer paradigm [65]. Some slight changes are made: (i) remove the causal mask in the image decoder; (ii) append the intermediate sequence prediction layers at end of image decoder. We use the MS COCO [37] dataset identical to DALL-Eval [8] for performance evaluation in all experiments. For more implementation details please refer to appendix A.

Like prior works [8, 65], we evaluate the text-to-image generation performance in two primary aspects: generated image quality, and alignment between generated image and input text. Specifically, the evaluation procedures are:

- *Image Quality*. Fréchet Inception Distance (FID) [21] is used as the primary automated metric for measuring image quality. Concretely, the FID score is computed by inputting generated and real images into the Inception v3 [55] network, and using the output of the

last pooling layer as extracted features. The features of the generated and real images are then used to fit two multi-variate Gaussians, respectively. Finally, the FID score is computed by measuring the Fréchet distance between these multi-variate Gaussian distributions.

- *Image-Text Alignment*. Text-image relation degree is estimated by automated captioning evaluation: an image output by the model is captioned with a standard trained Transformer-based model [9] and then the similarity of the input prompt and the generated caption is assessed via conventional metrics BLEU [40], CIDEr [60], METEOR [10], and SPICE [1].

4.1. Comparison with the state-of-the-art methods

In this part, the text-to-image generation performance of different methods is compared. Moreover, we introduce a text-to-image retrieval baseline, *i.e.*, given a text prompt, we retrieve the most matched image in the *training set*, measured by the cosine similarity between the text embedding and image embedding from pre-trained CLIP model [42].

Image Quality Evaluation. Following [47, 65], we use 30,000 generated and real image samples from MS COCO 2014 dataset for evaluation. Those images use the same input preprocessing with 256×256 image resolution. We compare our proposed models with several state-of-the-art methods, including autoregressive-based models X-LXMERT [7], minDALL-E [47], CogView [12], CogView 2 [13], RQ-Transformer [32], Parti [65], and diffusion-based models, DALL-E 2 [46] and Imagen [51]. The evaluation results coupled with the size of training data and model parameters are presented in Table 1. We can observe that our progressive model, which has similar parameter size to previous autoregressive-based models, achieves strongly competitive performance while posing an advance in inference speed. In particular, the progressive model shows strong generalization without fine-tuning on specific domains compared with miniDALL-E. Besides for scaling more parameters, the experiment results indicate that generation pattern exploration also holds promising potential for text-to-image creation.

Image-text Alignment Evaluation. The evaluation of image-text alignment complements the FID score for text-to-image generation models. Table 2 presents results of different models on the image-text alignment measurement. As expected, the progressive model outperforms other popular autoregressive-based models on this metric, and is close to the performance of retrieval-based baseline, which uses retrieval images for captioning. However, it should be noted that the results are biased due to the influence caused by the ability of pre-trained image captioning model [9].

| Approach | Model Type | # Data | # Param | MS COCO FID (\downarrow) | |
|--------------------|----------------|--------|---------|------------------------------|------------|
| | | | | Zero-shot | Fine-tuned |
| Retrieval Baseline | - | - | - | 19.12 | - |
| X-LXMERT | Autoregressive | 180K | 228M | 37.4 | - |
| DALL-E small | Autoregressive | 15M | 120M | 45.8 | - |
| minDALL-E | Autoregressive | 15M | 1.3B | 24.6 | - |
| CogView | Autoregressive | 30M | 4B | 27.1 | - |
| CogView2 | Autoregressive | 30M | 9B | 24.0 | 17.7 |
| RQ-Transformer | Autoregressive | 30M | 3.9B | 16.9 | - |
| DALL-E 2 | Diffusion | 650M | 5.5B | 10.39 | - |
| Imagen | Diffusion | 860M | 7.6B | 7.27 | - |
| Parti | Autoregressive | 800M | 20B | 7.23 | 3.22 |
| PTIG | Progressive | 20M | 1.2B | 13.28 | 5.34 |

Table 1. FID score comparison of different text-to-image synthesis models on the MS COCO dataset. Some listed evaluation results are from DALL-Eval and corresponding papers.

| Approach | BLEU (\uparrow) | METEOR (\uparrow) | CIDEr (\uparrow) | SPICE (\uparrow) |
|----------------------------|---------------------|-----------------------|----------------------|----------------------|
| Ground Truth (upper bound) | 32.5 | 27.5 | 108.3 | 20.4 |
| Retrieval Baseline | 22.4 | 21.7 | 81.5 | 15.3 |
| ruDALL-E-XL | 13.9 | 16.0 | 38.7 | 8.7 |
| minDALL-E | 16.6 | 17.6 | 48.0 | 10.5 |
| PTIG | 20.5 | 19.7 | 74.8 | 13.5 |

Table 2. Comparison for image captioning evaluation on the MS COCO test set.

| Order | FID (\downarrow) | CIDEr (\uparrow) |
|------------------|----------------------|----------------------|
| Left to right | 19.2 | 54.3 |
| Random | 20.1 | 51.2 |
| Anti-progressive | 22.2 | 49.5 |
| Const. Error | 16.1 | 64.3 |
| Progressive | 13.3 | 74.8 |

Table 3. Effects of different generation orders.

| # Stage | FID (\downarrow) | CIDEr (\uparrow) | SpeedUp |
|---------|----------------------|----------------------|---------------|
| 8 | 19.8 | 53.5 | 97.1 \times |
| 16 | 15.9 | 65.1 | 52.5 \times |
| 64 | 13.3 | 74.8 | 13.2 \times |
| 256 | 12.7 | 78.5 | 3.3 \times |
| 1024 | 12.5 | 79.8 | 1 \times |

Table 4. Effects of stage numbers.

4.2. Model Analysis

The Impact of Generation Order. To deeply analyze the effectiveness of generation order in text-to-image generation, we compare four different generation strategies under the same experiment setting. All baselines predict 16 image tokens at each stage, except for left-to-right manner which

predicts 1 image token each time. As shown in Table 3, we notice that the synthesis performance drops when replacing the progressive manner with the random or conventional sequence. This may indicate that predicting image tokens from coarse-to-fine benefits the quality of image generation. Furthermore, dynamic scoring-based order shows more advance than quantization error scoring and other baselines. Interestingly, we also train the model with anti-progressive order, *i.e.*, training model in a fine-to-coarse manner, and we can observe a significant reduction of performance, affirming the value of coarse-to-fine progressive generation manner again.

Number of Progressive Stages. One of the motivations of this work is that the generation can be parallel at each stage, leading to a significant reduction in training and inference time. To achieve the trade-off between inference speed and generation performance, we evaluate the models with different progressive stages. The acceleration evaluation is based on a single Nvidia V100 GPU in the MS COCO dataset. As shown in Table 4, we can find that when the stage number increases from 8 to 64, the performance improves prominently with slower inference speed. When it increases to 256, the generation performance reaches a plateau. Please note that the model with 1024 stages is

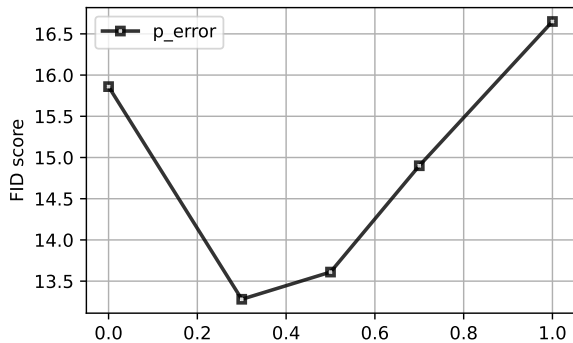


Figure 4. Effects of image token revision.

actually the autoregressive generation model with our dynamic scoring-based strategy. Therefore, we set the default stage number to 64 in our experiments for competitive performance and faster inference speed.

Effect of Image Token Revision. We investigate the influence of error revision in this section, where p_{error} is the probability of injecting pseudo incorrect image tokens to T training series for each instance. From the experiment results, we can observe that: (i) without the error revision, i.e., $p_{error} = 0$, the FID score increases significantly, indicating that the error revision mechanism is effective for performance improvement. (ii) As p_{error} becomes larger, the performance becomes improved at first and deteriorated thereafter. We believe that too many pseudo errors make it hard to learn the correct text-to-image mapping. (iii) The model achieves best performance with $p_{error} = 0.3$, which is set as default value in other experiments.

4.3. Cases from Progressive Model

To demonstrate the capability of generating in-the-wild images, we provide some generated results in Figure 2 and more intuitive cases comparison can be found in Appendix B. Though our base model is much smaller than previous works like Parti, we also achieve a promising performance with some delicate design. Compared with the AR methods which generate images from top-left to down-right, our method generates images in a global manner and supports error revision timely, resulting in much more high-quality and content-rich images. We also list some bad cases in Figure 5 to provide insights on how our approach may be improved. These cases show representative types of errors, i.e., negative semantic understanding, and spatial relations. Although our approach generates unfavorable images, it still generates related subjects.

4.4. Human Evaluation

We follow the form in [65] to conduct side-by-side human evaluations for minDALL-E, Random vs. our progressive model from image realism and image-text match aspects. Please note that compared with minDALL-E, the model with random generation mode uses image token revision. Detailed setting please refer to appendix C. The evaluation results are summarized in Table 5. As we can see, our progressive model outperforms minDALL-E, which is the popular open-source autoregressive image generation model and holds a similar model parameter and training data size. When compared against the random mode with the same network architecture, our progressive model still shows superiority for optimized generation order.

5. Related Works

Autoregressive Image Synthesis. Currently, autoregressive models [43, 44] have shown promising results for text-to-image generation [6, 16, 41, 48, 57, 58]. Prior works including PixelRNN [58], Image Transformer [41] and ImageGPT [6] factorize the conditional probability on an image over raw pixels. Due to the intolerable amount of computation for large images, modeling images in the low-dimension discrete latent space is introduced. VQ-VAE, VQ-GAN, and ImageBART [15] train an encoder to compress the image and fit the density of the hidden variables. It greatly improves the performance of image generation. More recent DALL-E [46], CogView [12], M6 [36], ERINE-ViLG [66], and Parti [65] all utilize AR-based Transformer architectures in the latent space. Similarly, [33] consider global image information with refinement by random masking. With a powerful large transformer structure and massive text-image pairs, they greatly advance the quality of text-to-image generation yet still ignore the importance and order of image tokens.

Denosing Diffusion Probabilistic. Another related work for text-to-image generation is deep diffusion model, which is first proposed in [53] and achieved strong results on audio [26, 31], image [11, 22, 23, 39, 50], video [24] generation, and super super-resolution [52]. Discrete diffusion models are also first described in [53], and then applied to text generation [2, 25]. D3PMs [2] introduce discrete diffusion to image generation. As directly estimating the density of raw image pixels can only generate low-resolution images, more recent works [20, 34, 49, 61] resort to diffuse in the VQ-based latent space.

6. Conclusion

In this paper, we propose that the generation order of image tokens are important for text-to-image generation. To

| | Image Realism | | | Image-Text Match | | |
|-----------|---------------|--------|------------|------------------|--------|------------|
| | baseline wins | border | prog. wins | baseline wins | border | prog. wins |
| minDALL-E | 34.3 | 24.2 | 41.5 | 33.0 | 31.2 | 35.8 |
| Random | 31.2 | 29.7 | 39.2 | 33.7 | 27.8 | 38.5 |

Table 5. Human evaluation results over 200 textual prompts and the corresponding generated images from the MS COCO test set.



Figure 5. Images generated from progressive model showing errors in *number counting and negative semantic understanding*, which motivates the future improvement.

this end, we introduce a progressive model, which builds the image sequence in a coarse-to-fine manner according to variant scoring strategies. The resulting top-down hierarchy makes the generation process interpretable and enjoys a significant reduction over empirical time. Moreover, we seamlessly integrate the component of image token revision into our progressive framework, which further improves the model performance. Extensive experiments show that our progressive model can produce more perceptually appealing samples and better evaluation metrics than conventional autoregressive models. More encouragingly, our model achieves much faster inference speed, and is looking forward to be applied to various practical applications.

References

- [1] Peter Anderson, Basura Fernando, Mark Johnson, and Stephen Gould. Spice: Semantic propositional image caption evaluation. In *European conference on computer vision*, pages 382–398. Springer, 2016. 6
- [2] Jacob Austin, Daniel D Johnson, Jonathan Ho, Daniel Tarlow, and Rianne van den Berg. Structured denoising diffusion models in discrete state-spaces. *Advances in Neural Information Processing Systems*, 34:17981–17993, 2021. 8
- [3] Sam Bond-Taylor, Adam Leach, Yang Long, and Chris G Willcocks. Deep generative modelling: A comparative review of vaes, gans, normalizing flows, energy-based and autoregressive models. *IEEE transactions on pattern analysis and machine intelligence*, 2021. 2
- [4] Tom Brown, Benjamin Mann, Nick Ryder, Melanie Subbiah, Jared D Kaplan, Prafulla Dhariwal, Arvind Neelakantan, Pranav Shyam, Girish Sastry, Amanda Askell, et al. Language models are few-shot learners. *Advances in neural information processing systems*, 33:1877–1901, 2020. 2
- [5] Soravit Changpinyo, Piyush Sharma, Nan Ding, and Radu Soricut. Conceptual 12m: Pushing web-scale image-text pre-training to recognize long-tail visual concepts. In *Proceedings of the IEEE/CVF Conference on Computer Vision and Pattern Recognition*, pages 3558–3568, 2021. 2
- [6] Mark Chen, Alec Radford, Rewon Child, Jeffrey Wu, Heewoo Jun, David Luan, and Ilya Sutskever. Generative pre-training from pixels. In *International conference on machine learning*, pages 1691–1703. PMLR, 2020. 2, 8
- [7] Jaemin Cho, Jiasen Lu, Dustin Schwenk, Hannaneh Hajishirzi, and Aniruddha Kembhavi. X-ixmert: Paint, caption and answer questions with multi-modal transformers. In *Proceedings of the 2020 Conference on Empirical Methods in Natural Language Processing*, pages 8785–8805, 2020. 6
- [8] Jaemin Cho, Abhay Zala, and Mohit Bansal. Dall-eval: Probing the reasoning skills and social biases of text-to-image generative transformers. *arXiv preprint arXiv:2202.04053*, 2022. 6
- [9] Marcella Cornia, Matteo Stefanini, Lorenzo Baraldi, and Rita Cucchiara. Meshed-memory transformer for image captioning. In *Proceedings of the IEEE/CVF conference on computer vision and pattern recognition*, pages 10578–10587, 2020. 6
- [10] Michael Denkowski and Alon Lavie. Meteor universal: Language specific translation evaluation for any target language. In *Proceedings of the ninth workshop on statistical machine translation*, pages 376–380, 2014. 6
- [11] Prafulla Dhariwal and Alexander Nichol. Diffusion models beat gans on image synthesis. *Advances in Neural Information Processing Systems*, 34:8780–8794, 2021. 2, 8
- [12] Ming Ding, Zhuoyi Yang, Wenyi Hong, Wendi Zheng, Chang Zhou, Da Yin, Junyang Lin, Xu Zou, Zhou Shao, Hongxia Yang, et al. Cogview: Mastering text-to-image generation via transformers. *Advances in Neural Information Processing Systems*, 34:19822–19835, 2021. 2, 4, 6, 8

- [13] Ming Ding, Wendi Zheng, Wenyi Hong, and Jie Tang. Cogview2: Faster and better text-to-image generation via hierarchical transformers. *arXiv preprint arXiv:2204.14217*, 2022. 6
- [14] Xiaoyi Dong, Jianmin Bao, Ting Zhang, Dongdong Chen, Weiming Zhang, Lu Yuan, Dong Chen, Fang Wen, and Nenghai Yu. Peco: Perceptual codebook for bert pre-training of vision transformers. *arXiv preprint arXiv:2111.12710*, 2021. 5
- [15] Patrick Esser, Robin Rombach, Andreas Blattmann, and Bjorn Ommer. Imagebart: Bidirectional context with multinomial diffusion for autoregressive image synthesis. *Advances in Neural Information Processing Systems*, 34:3518–3532, 2021. 8
- [16] Patrick Esser, Robin Rombach, and Bjorn Ommer. Taming transformers for high-resolution image synthesis. In *Proceedings of the IEEE/CVF conference on computer vision and pattern recognition*, pages 12873–12883, 2021. 2, 4, 6, 8, 13
- [17] Oran Gafni, Adam Polyak, Oron Ashual, Shelly Sheynin, Devi Parikh, and Yaniv Taigman. Make-a-scene: Scene-based text-to-image generation with human priors. *arXiv preprint arXiv:2203.13131*, 2022. 2
- [18] Jiatao Gu, James Bradbury, Caiming Xiong, Victor OK Li, and Richard Socher. Non-autoregressive neural machine translation. In *International Conference on Learning Representations*, 2018. 6
- [19] Jiatao Gu and Xiang Kong. Fully non-autoregressive neural machine translation: Tricks of the trade. In *Findings of the Association for Computational Linguistics: ACL-IJCNLP 2021*, pages 120–133, 2021. 6
- [20] Shuyang Gu, Dong Chen, Jianmin Bao, Fang Wen, Bo Zhang, Dongdong Chen, Lu Yuan, and Baining Guo. Vector quantized diffusion model for text-to-image synthesis. In *Proceedings of the IEEE/CVF Conference on Computer Vision and Pattern Recognition*, pages 10696–10706, 2022. 4, 8
- [21] Martin Heusel, Hubert Ramsauer, Thomas Unterthiner, Bernhard Nessler, and Sepp Hochreiter. Gans trained by a two time-scale update rule converge to a local nash equilibrium. *Advances in neural information processing systems*, 30, 2017. 6
- [22] Jonathan Ho, Ajay Jain, and Pieter Abbeel. Denoising diffusion probabilistic models. *Advances in Neural Information Processing Systems*, 33:6840–6851, 2020. 2, 8
- [23] Jonathan Ho, Chitwan Saharia, William Chan, David J Fleet, Mohammad Norouzi, and Tim Salimans. Cascaded diffusion models for high fidelity image generation. *J. Mach. Learn. Res.*, 23:47–1, 2022. 8
- [24] Jonathan Ho, Tim Salimans, Alexey A Gritsenko, William Chan, Mohammad Norouzi, and David J Fleet. Video diffusion models. In *ICLR Workshop on Deep Generative Models for Highly Structured Data*, 2022. 8
- [25] Emiel Hoogeboom, Didrik Nielsen, Priyank Jaini, Patrick Forré, and Max Welling. Argmax flows and multinomial diffusion: Towards non-autoregressive language models. 2021. 8
- [26] Myeonghun Jeong, Hyeongju Kim, Sung Jun Cheon, Byoung Jin Choi, and Nam Soo Kim. Diff-tts: A denoising diffusion model for text-to-speech. *arXiv preprint arXiv:2104.01409*, 2021. 8
- [27] Chao Jia, Yinfei Yang, Ye Xia, Yi-Ting Chen, Zarana Parekh, Hieu Pham, Quoc Le, Yun-Hsuan Sung, Zhen Li, and Tom Duerig. Scaling up visual and vision-language representation learning with noisy text supervision. In *International Conference on Machine Learning*, pages 4904–4916. PMLR, 2021. 2
- [28] Andrej Karpathy and Li Fei-Fei. Deep visual-semantic alignments for generating image descriptions. In *Proceedings of the IEEE conference on computer vision and pattern recognition*, pages 3128–3137, 2015. 13
- [29] Jacob Devlin Ming-Wei Chang Kenton and Lee Kristina Toutanova. Bert: Pre-training of deep bidirectional transformers for language understanding. In *Proceedings of NAACL-HLT*, pages 4171–4186, 2019. 4
- [30] Diederik P Kingma and Jimmy Ba. Adam: A method for stochastic optimization. *arXiv preprint arXiv:1412.6980*, 2014. 13
- [31] Zhifeng Kong, Wei Ping, Jiayi Huang, Kexin Zhao, and Bryan Catanzaro. Diffwave: A versatile diffusion model for audio synthesis. In *International Conference on Learning Representations*, 2020. 8
- [32] Doyup Lee, Chiheon Kim, Saehoon Kim, Minsu Cho, and Wook-Shin Han. Autoregressive image generation using residual quantization. In *Proceedings of the IEEE/CVF Conference on Computer Vision and Pattern Recognition*, pages 11523–11532, 2022. 2, 6
- [33] Doyup Lee, Chiheon Kim, Saehoon Kim, Minsu Cho, and Wook-Shin Han. Draft-and-revise: Effective image generation with contextual rq-transformer. *arXiv preprint arXiv:2206.04452*, 2022. 8
- [34] Sangyun Lee, Hyungjin Chung, Jaehyeon Kim, and Jong Chul Ye. Progressive deblurring of diffusion models for coarse-to-fine image synthesis. *arXiv preprint arXiv:2207.11192*, 2022. 4, 8
- [35] Junnan Li, Ramprasaath Selvaraju, Akhilesh Gotmare, Shafiq Joty, Caiming Xiong, and Steven Chu Hong Hoi. Align before fuse: Vision and language representation learning with momentum distillation. *Advances in neural information processing systems*, 34:9694–9705, 2021. 2
- [36] Junyang Lin, Rui Men, An Yang, Chang Zhou, Ming Ding, Yichang Zhang, Peng Wang, Ang Wang, Le Jiang, Xianyan Jia, et al. M6: A chinese multimodal pretrainer. *arXiv preprint arXiv:2103.00823*, 2021. 8
- [37] Tsung-Yi Lin, Michael Maire, Serge Belongie, James Hays, Pietro Perona, Deva Ramanan, Piotr Dollár, and C Lawrence Zitnick. Microsoft coco: Common objects in context. In *European conference on computer vision*, pages 740–755. Springer, 2014. 2, 6, 13
- [38] Alex Nichol, Prafulla Dhariwal, Aditya Ramesh, Pranav Shyam, Pamela Mishkin, Bob McGrew, Ilya Sutskever, and Mark Chen. Glide: Towards photorealistic image generation and editing with text-guided diffusion models. *arXiv preprint arXiv:2112.10741*, 2021. 2

- [39] Alexander Quinn Nichol and Prafulla Dhariwal. Improved denoising diffusion probabilistic models. In *International Conference on Machine Learning*, pages 8162–8171. PMLR, 2021. 8
- [40] Kishore Papineni, Salim Roukos, Todd Ward, and Wei-Jing Zhu. Bleu: a method for automatic evaluation of machine translation. In *Proceedings of the 40th annual meeting of the Association for Computational Linguistics*, pages 311–318, 2002. 6
- [41] Niki Parmar, Ashish Vaswani, Jakob Uszkoreit, Lukasz Kaiser, Noam Shazeer, Alexander Ku, and Dustin Tran. Image transformer. In *International conference on machine learning*, pages 4055–4064. PMLR, 2018. 8
- [42] Alec Radford, Jong Wook Kim, Chris Hallacy, Aditya Ramesh, Gabriel Goh, Sandhini Agarwal, Girish Sastry, Amanda Askell, Pamela Mishkin, Jack Clark, et al. Learning transferable visual models from natural language supervision. In *International Conference on Machine Learning*, pages 8748–8763. PMLR, 2021. 2, 5, 6
- [43] Alec Radford, Karthik Narasimhan, Tim Salimans, Ilya Sutskever, et al. Improving language understanding by generative pre-training. 2018. 8
- [44] Alec Radford, Jeffrey Wu, Rewon Child, David Luan, Dario Amodei, Ilya Sutskever, et al. Language models are unsupervised multitask learners. *OpenAI blog*, 1(8):9, 2019. 8
- [45] Colin Raffel, Noam Shazeer, Adam Roberts, Katherine Lee, Sharan Narang, Michael Matena, Yanqi Zhou, Wei Li, Peter J Liu, et al. Exploring the limits of transfer learning with a unified text-to-text transformer. *J. Mach. Learn. Res.*, 21(140):1–67, 2020. 4, 13
- [46] Aditya Ramesh, Prafulla Dhariwal, Alex Nichol, Casey Chu, and Mark Chen. Hierarchical text-conditional image generation with clip latents. *arXiv preprint arXiv:2204.06125*, 2022. 2, 6, 8
- [47] Aditya Ramesh, Mikhail Pavlov, Gabriel Goh, Scott Gray, Chelsea Voss, Alec Radford, Mark Chen, and Ilya Sutskever. Zero-shot text-to-image generation. In *International Conference on Machine Learning*, pages 8821–8831. PMLR, 2021. 2, 4, 6
- [48] Ali Razavi, Aaron Van den Oord, and Oriol Vinyals. Generating diverse high-fidelity images with vq-vae-2. *Advances in neural information processing systems*, 32, 2019. 8
- [49] Robin Rombach, Andreas Blattmann, Dominik Lorenz, Patrick Esser, and Bjorn Ommer. High-resolution image synthesis with latent diffusion models. In *Proceedings of the IEEE/CVF Conference on Computer Vision and Pattern Recognition*, pages 10684–10695, 2022. 2, 4, 8
- [50] Chitwan Saharia, William Chan, Huiwen Chang, Chris Lee, Jonathan Ho, Tim Salimans, David Fleet, and Mohammad Norouzi. Palette: Image-to-image diffusion models. In *ACM SIGGRAPH 2022 Conference Proceedings*, pages 1–10, 2022. 8
- [51] Chitwan Saharia, William Chan, Saurabh Saxena, Lala Li, Jay Whang, Emily Denton, Seyed Kamyar Seyed Ghasemipour, Burcu Karagol Ayan, S Sara Mahdavi, Rapha Gontijo Lopes, et al. Photorealistic text-to-image diffusion models with deep language understanding. *arXiv preprint arXiv:2205.11487*, 2022. 2, 6
- [52] Chitwan Saharia, Jonathan Ho, William Chan, Tim Salimans, David J Fleet, and Mohammad Norouzi. Image super-resolution via iterative refinement. *arXiv preprint arXiv:2104.07636*, 2021. 8
- [53] Jascha Sohl-Dickstein, Eric Weiss, Niru Maheswaranathan, and Surya Ganguli. Deep unsupervised learning using nonequilibrium thermodynamics. In *International Conference on Machine Learning*, pages 2256–2265. PMLR, 2015. 8
- [54] Richard S Sutton, David McAllester, Satinder Singh, and Yishay Mansour. Policy gradient methods for reinforcement learning with function approximation. *Advances in neural information processing systems*, 12, 1999. 6
- [55] Christian Szegedy, Vincent Vanhoucke, Sergey Ioffe, Jon Shlens, and Zbigniew Wojna. Rethinking the inception architecture for computer vision. In *Proceedings of the IEEE conference on computer vision and pattern recognition*, pages 2818–2826, 2016. 6
- [56] Bowen Tan, Zichao Yang, Maruan Al-Shedivat, Eric Xing, and Zhiting Hu. Progressive generation of long text with pre-trained language models. In *Proceedings of the 2021 Conference of the North American Chapter of the Association for Computational Linguistics: Human Language Technologies*, pages 4313–4324, 2021. 2
- [57] Aaron Van Den Oord, Oriol Vinyals, et al. Neural discrete representation learning. *Advances in neural information processing systems*, 30, 2017. 2, 8
- [58] Aaron Van Oord, Nal Kalchbrenner, and Koray Kavukcuoglu. Pixel recurrent neural networks. In *International conference on machine learning*, pages 1747–1756. PMLR, 2016. 8
- [59] Ashish Vaswani, Noam Shazeer, Niki Parmar, Jakob Uszkoreit, Llion Jones, Aidan N Gomez, Łukasz Kaiser, and Illia Polosukhin. Attention is all you need. *Advances in neural information processing systems*, 30, 2017. 2
- [60] Ramakrishna Vedantam, C Lawrence Zitnick, and Devi Parikh. Cider: Consensus-based image description evaluation. In *Proceedings of the IEEE conference on computer vision and pattern recognition*, pages 4566–4575, 2015. 6
- [61] Zihao Wang, Wei Liu, Qian He, Xinglong Wu, and Zili Yi. Clip-gen: Language-free training of a text-to-image generator with clip. *arXiv preprint arXiv:2203.00386*, 2022. 4, 8
- [62] Chenfei Wu, Jian Liang, Xiaowei Hu, Zhe Gan, Jianfeng Wang, Lijuan Wang, Zicheng Liu, Yuejian Fang, and Nan Duan. Nuwa-infinity: Autoregressive over autoregressive generation for infinite visual synthesis. *arXiv preprint arXiv:2207.09814*, 2022. 2
- [63] Jiahui Yu, Xin Li, Jing Yu Koh, Han Zhang, Ruoming Pang, James Qin, Alexander Ku, Yuanzhong Xu, Jason Baldridge, and Yonghui Wu. Vector-quantized image modeling with improved vqgan. *arXiv preprint arXiv:2110.04627*, 2021. 2
- [64] Jiahui Yu, Zirui Wang, Vijay Vasudevan, Legg Yeung, Mojtaba Seyedhosseini, and Yonghui Wu. Coca: Contrastive captioners are image-text foundation models. *arXiv preprint arXiv:2205.01917*, 2022. 2

- [65] Jiahui Yu, Yuanzhong Xu, Jing Yu Koh, Thang Luong, Gungjan Baid, Zirui Wang, Vijay Vasudevan, Alexander Ku, Yinfei Yang, Burcu Karagol Ayan, et al. Scaling autoregressive models for content-rich text-to-image generation. *arXiv preprint arXiv:2206.10789*, 2022. [2](#), [4](#), [6](#), [8](#), [13](#)
- [66] Han Zhang, Weichong Yin, Yewei Fang, Lanxin Li, Boqiang Duan, Zhihua Wu, Yu Sun, Hao Tian, Hua Wu, and Haifeng Wang. Ernie-vilg: Unified generative pre-training for bidirectional vision-language generation. *arXiv preprint arXiv:2112.15283*, 2021. [8](#)

A. Experimental Settings

Datasets for Training and Evaluation. We train on a combination of image-text datasets for progressive model training, including a filtered subset of LAION-400M and Conceptual Captions-3M. For all image inputs, we follow the VQ-GAN [16] input processing with weight trained on ImageNet to pre-extract the image token sequence. To demonstrate the capability of our proposed method for text-to-image synthesis, we conduct experiments on the MS COCO dataset [37], which currently is a standard benchmark for text-to-image performance evaluation. MS COCO dataset contains 82k images for training and 40k images for testing. Each image in this dataset has five human-annotated text descriptions. In this paper, we conduct experiments consistent with Karpathy split [28].

Implementation Details. For the image tokenizer, we follow the setting of original VQ-GAN [16], which leverages the GAN loss to get a more realistic image. The codebook size is 163,84 with a dimension of 256, and a compression ratio of 16. That is, it converts 512×512 images into 32×32 tokens. We directly adopt the publicly available VQ-GAN model trained on the ImageNet dataset for all text-to-image synthesis experiments from <https://github.com/CompVis/taming-transformers>. We adopt a publicly available tokenizer of the base version of t5 [45] as a text encoder. For the decoder of the text-to-image transformer, we set the stacked layer number to 24, the hidden dimension to 1280, the feed-forward dimension to 4096, and the head number to 20. An additional linear layer is appended at the last transformer layer to predict the state sequence. For error revision data construction, we select $p_{error} = 0.3$ with a fixed 15% replaced ratio of available tokens in the current sequence by default. Besides, more advanced strategies for pseudo image token selection are left for future work. Both image and text encoders in our training process are frozen. We use AdamW [30] optimizer with $\beta_1 = 0.9$ and $\beta_2 = 0.96$. The model is trained for 120 epochs with the cosine learning rate schedule with the initial value of $1e-4$.

B. More Cases Analysis

To illustrate the performance of the proposed progressive model more intuitively, we also compared it with the most popular VQ-AR based minDALL-E model. The generated images can be seen in Figure 6, where the input text prompts are from the MS COCO dataset. We can observe that the results of the progressive model are more fine-grained, more harmonious from a global perspective, and the semantics controls are more accurate.

C. Human Evaluation

We follow [65] to conduct side-by-side human evaluations, in which well-educated human annotators are presented with two outputs for the same prompt and are asked to choose which image is a higher quality and more natural image (image realism) and which is a better match to the input prompt (image-text alignment). As for the Turing test, the model types are anonymized and randomly shuffled for each presentation to an annotator, and each pair is judged by three independent annotators. The results are summarized in Table 5. Finally, annotators have received reasonable remuneration for their labor.



a black Honda motorcycle parked in front of a garage



a room with blue walls and a white sink and door



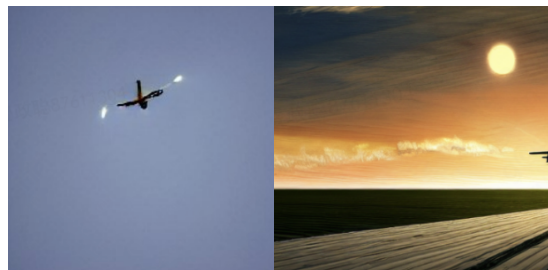
an old-fashioned green station wagon is parked on a shady driveway



a cute kitten is sitting in a dish on a table



fruit in a jar filled with liquid sitting on a wooden table



a striped plane flying up into the sky as the sun shines behind it

Figure 6. Image samples generated from minDALL-E in the left and our progressive model in the right, equipped with input text prompts from MS COCO dataset.